Effect of Hydrogen on Mode II Fatigue Behavior of Bearing Steel under Cyclic Torsion with Compressive Mean Stress

Shinji Fujita[1, a], Saburo Matsuoka[2, b] and Yukitaka Murakami[2, c]

[1] NSK Ltd. Currently at Graduate School of Engineering, Kyushu University, Moto-oka, Nishi-ku, Fukuoka 819-0395, Japan

[2] Kyushu University and The Research Center for Hydrogen Industrial Use and Storage (HYDROGENIUS), AIST, Moto-oka, Nishi-ku, Fukuoka 819-0395, Japan

[a] fujitash@mech.kyushu-u.ac.jp, [b] smatuoka@mech.kyushu-u.ac.jp, [c] ymura@mech.kyushu-u.ac.jp

Keywords: Bearing Steel, Multiaxial Fatigue, Cyclic Torsion with Static Compression, Mode II Fatigue Crack, Hydrogen, Microstructural Change, White Structure Flaking

Abstract. In order to investigate effect of hydrogen on Mode II fatigue behavior, fatigue tests were conducted using hydrogen-precharged and uncharged specimens of bearing steel (SAE 52100, *HV*=748) tempered at 438K loaded under cyclic torsion with and without a compressive mean stress (σ_m=0, -750MPa). The fatigue lives were shorter in the hydrogen-precharged specimens than in the uncharged specimens loaded under cyclic torsion with and without a compressive mean stress. In both hydrogen-precharged and uncharged specimens, Mode II fatigue cracks initiated and propagated along the axial direction of specimen due to the longitudinal microstructure texture formed in the rolling direction. Mode II fatigue crack growth rate and Mode I fatigue crack growth rate of the hydrogen-precharged specimens were higher than those of uncharged specimens under the compression-torsion test. More mode II fatigue cracks were observed at the final stage (N/N_f=0.97) in the hydrogen-precharged specimen than in the uncharged specimen. Microstructural changes were observed only in the hydrogen-precharged specimens. From these observations, it is presumed that hydrogen enhances slip deformation and localized slip bands, and eventually produces more mode II fatigue cracks along slip bands in the hydrogen-precharged specimens.

Introduction

Fatigue failure in the rolling bearing is called flaking. Mode II fatigue crack growth plays an important role in flaking. Recently, it is reported that premature flaking occurs in rolling bearings used in electrical engine-driven accessories such as alternators [1, 2]. This premature flaking is called white structure flaking because the microstructural change (white structure) is observed in failured bearings. White structure flaking is thought to occur by the effect of hydrogen [3, 4].

The objective of the present paper is to investigate effect of hydrogen on Mode II fatigue crack behavior. Fatigue tests were conducted using hydrogen-precharged and uncharged specimens loaded under cyclic torsion with and without a compressive mean stress (σ_m=0, -750MPa). In particular, in order to investigate effects of hydrogen on Mode II fatigue crack initiation and growth behavior, fatigue tests were conducted under cyclic torsion with a compressive mean stress. The replica method and scanning electron microscope (SEM) were used for observing crack extension.

Table1 Chemical composition of the material, mass%.

	C	Si	Mn	P	S	Ni	Cr	Mo	Cu	O (ppm)	Ti (ppm)
SUJ2	0.98	0.23	0.36	0.014	0.003	0.05	1.41	0.02	0.09	5	130

Experimental procedure

Round bars of SAE52100 were used in this study. Table 1 shows the chemical composition of the material. Figure 1 shows the shape and dimensions of fatigue test specimens machined from bars with a diameter of 23 mm. They were oil quenched from 1113K and followed by tempering at 438K. The

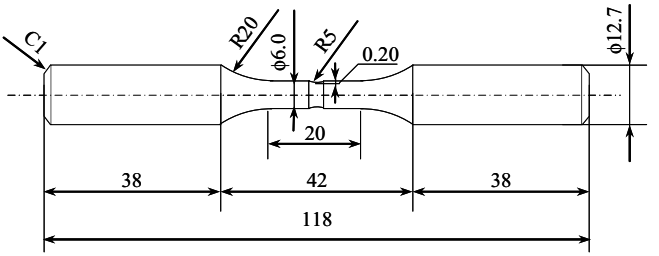

FIGURE 1 The shape of fatigue test specimens (Dimension in mm).

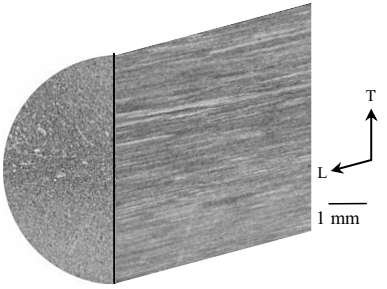

FIGURE 2 Microstructure of the material.

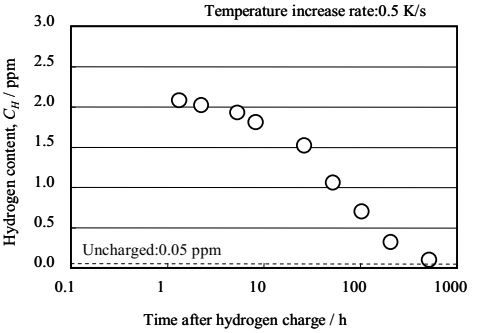

FIGURE 3 The variation in hydrogen content after hydrogen charge.

specimen surface was finished with buffing after polishing with emery paper #2000. The notch radius was 5 mm and notch depth was 0.2 mm. This notch was introduced in order to localize the crack initiation. The stress concentration factor of the notch was K_t=1.38 for axial loading and K_t=1.08 for torsion. The Vickers hardness was *HV* 748 (the average of 20 measurements with a measurement load of 2.94 N). Scatter of *HV* measured was within 2%. Figure 2 shows the microstructure. Longitudinal microstructure texture is formed in the rolling direction. Hydrogen was charged by soaking specimens in an aqueous solution of 20 mass% NH_4SCN at 313 K for 24 hours. Hydrogen content in specimens was measured by thermal desorption spectrometry (TDS) up to 773K at the heating rate of 0.5K/s. Figure 3 shows the variations in hydrogen content with time after a hydrogen charge. Hydrogen was initially charged into a rolled bar with a diameter of 6 mm and then a 2.0-mm-thick disk was cut out form the bar for the TDS measurement. Fatigue tests were carried out at room temperature in laboratory air using a biaxial servo-hydraulic fatigue testing machine. Tests condition consist of nominal shear stress amplitudes, τ_a=700~1300 MPa, nominal compressive mean stresses, σ_m=0 and -750 MPa, frequencies, f=1.0~3.5 Hz, and stress ratio, R=-1. Nominal shear stress τ_a is defined by $16T/\pi d^3$, even though yielding occurs at the specimen surface of some specimens. The hydrogen-precharged specimens were re-polished before fatigue tests to remove flaws produced by hydrogen charge. Fatigue tests were started within 4 h from the hydrogen charge. In order to measure the hydrogen content, 2.0-mm-thick disks were immediately cut out from each specimen, under water

cooling. Fatigue cracks were observed by the replica method. Microstructural changes were examined using SEM at an acceleration voltage of 20 kV.

Results and Discussion

Effect of compressive mean stress and hydrogen on S-N property

Figure 4 shows *S-N* data for the uncharged specimens and the hydrogen-precharged specimens with and without a compressive mean nominal stress. The hydrogen content of the hydrogen-precharged specimens, which was measured immediately after fatigue test, and fracture origin of the uncharged and hydrogen-precharged specimens are also including in the figure. As shown in Figure 4(a), fatigue lives N_f in the hydrogen-precharged specimens were shorter by a factor of more than 1/10 compared to those in the uncharged specimens under the cyclic torsion without a compressive mean stress (pure torsion test). The fracture origin was in the matrix at the surface for all uncharged specimens. One fracture occurred in the matrix and the remainder fracture from subsurface inclusion (Al_2O_3·CaO) in the hydrogen-precharged specimens.

Murakami *et al.* [5] pointed out the effect of hydrogen on subsurface inclusion originated fracture under tension-compression fatigue tests of SCM435 Cr-Mo steel (carbonitriding heat treatment, surface hardness: *HV*=780). They also found that fatigue lives N_f were shorter in hydrogen-precharged specimens than in uncharged specimens. The results of Murakami *et al.* suggest that hydrogen enhanced concentration of plastic deformation at subsurface inclusion and crack initiation followed by Mode I fracture under pure torsion fatigue tests of SAE52100. Fatigue lives N_f of specimens which fractured from the matrix were shorter in hydrogen-precharged specimens under the pure torsion test. This is because enhanced slip deformation and localized slip bands due to the hydrogen produce microstructural changes which are described in a later section.

As shown in Figure 4(b), fatigue lives N_f was shorter by factors of 1/2~1/8 in hydrogen-precharged specimens than in uncharged specimens under cyclic torsion with a compressive mean stress, σ_m=-750 MPa (compression-torsion test). The fracture origin was a surface inclusion (TiN) for four uncharged specimens and the matrix for one uncharged specimen. On the other hand, all five hydrogen-precharged specimens showed a matrix failure origin. The fracture origin in the uncharged specimens was changed from a matrix to a surface inclusion due to compressive mean stress. The plastic strain at the interface between inclusion and matrix is higher under the compression-torsion test than under the pure torsion test. As a result, it is presumed that the higher plastic strain under the compression-torsion test debonded the interface between inclusion and matrix. Thus, fatigue cracks initiated from the deponded inclusion (i.e. the defect) in the uncharged specimens under cyclic torsion with a compressive mean stress.

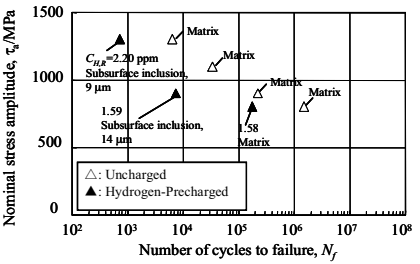

(a) Under cyclic torsion without a compressive mean stress (σ_m=0 MPa, f=1~3.0 Hz).

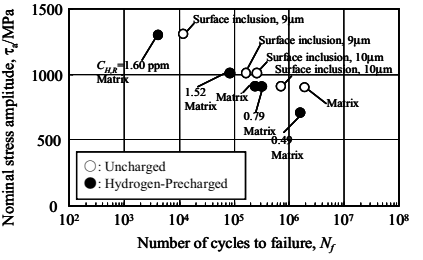

(b) Under cyclic torsion combined with a compressive mean stress (σ_m=-750 MPa, f=1~3.5 Hz).

FIGURE 4 *S-N* data for the uncharged and hydrogen-precharged specimens of SAE52100 under cyclic torsion with and without a compressive mean stress.

Fatigue lives of the specimens in both the uncharged and the hydrogen-precharged condition were 2 ~ 10 times longer with a compressive axial stress. The compressive mean stress acts on Mode I crack faces, delayed the branching from Mode II to Mode I. As a result, fatigue lives in both uncharged and hydrogen-precharged specimens increase with a compressive axial stress.

Effect of hydrogen on Mode II fatigue crack initiation and growth behavior

Figure 5 shows fatigue crack morphologies on the specimen surfaces for the uncharged and the hydrogen-precharged specimens under compression-torsion test with τ_a=1000 MPa. Black arrows show the main cracks, white arrows show the retained cracks. More Mode II cracks were observed at the final stage (N/N_f=0.97) in the hydrogen-precharged specimen than in the uncharged specimen. The similar morphology was observed in the hydrogen-precharged specimen at τ_a=700~1000 MPa.

Uyama *et al.* [6] explained the effect of hydrogen on the surface morphology of 0.45 % carbon steel (*HV*=185) with the ferrite-pearlite microstructure in the tension-compression fatigue test. They found that many slip bands and cracks were formed in the ferrite grains because hydrogen enhanced the localization of slip deformation. The results of Uyama *et al.* suggest that many slip bands are formed and many cracks are generated along slip bands even in the high strength steel SAE52100 (*HV*=748) in a tempered martensite microstructure by the slip localization due to the hydrogen.

Figure 6 shows typical crack initiation and growth for the uncharged and hydrogen-precharged specimens with a nominal shear stress amplitude τ_a=900 MPa in pure torsion test (σ_m=0 MPa) and compression-torsion test (σ_m=-750 MPa). Fatigue cracks initiated from subsurface inclusions in the hydrogen-precharged specimen in the pure torsion test (Figure 6(a-2)), and from surface inclusion in the uncharged specimen in the compression-torsion test (Figure 6(b-1)). The fracture origin was in the matrix under the other test conditions. Mode II cracks initiated and grew along the axial direction. Then, Mode II cracks branched into two Mode I cracks in the ± 45° direction. Mode I cracks continued propagation and led the specimen to failure. Zhang and Akid [7] showed that Mode II crack initiation along the axial direction of specimen was due to the

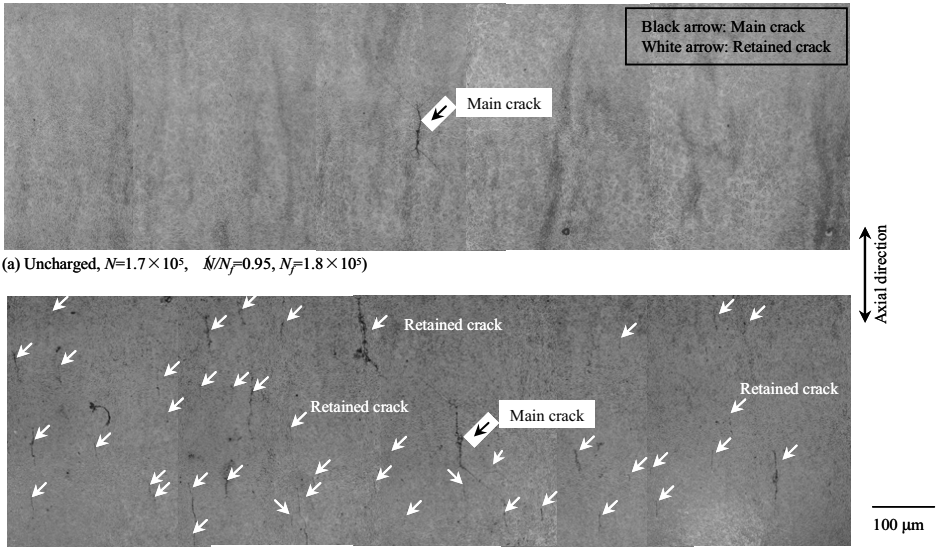

(a) Uncharged, N=1.7×10^5, (N/N_f=0.95, N_f=1.8×10^5)

(b) Hydrogen-precharged, N=8.5×10^4, (N/N_f=0.97, N_f=8.8×10^4), $C_{H,R}$=1.52 ppm

FIGURE 5 Fatigue cracks morphologies of the uncharged and hydrogen-precharged specimens of SAE52100 under cyclic torsion with a compressive mean stress (σ_m=-750 MPa, τ_a= 1000 MPa, f=3 Hz). $C_{H,R}$: Residual hydrogen content.

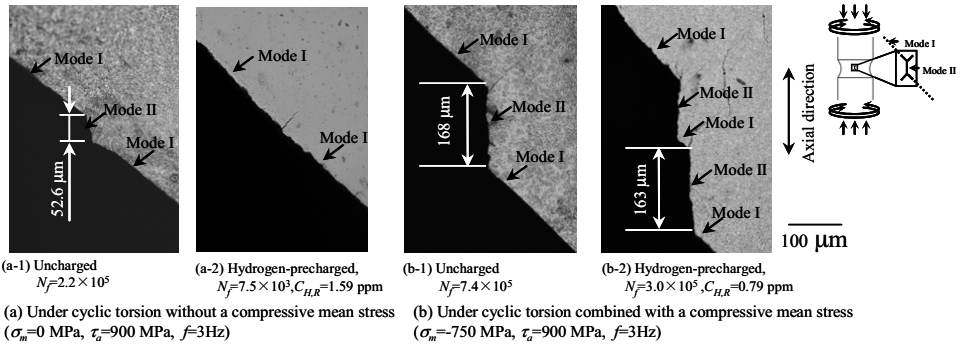

FIGURE 6 Fracture morphologies of the uncharged and hydrogen-precharged specimens of SAE52100 under cyclic torsion with and without a compressive mean stress. $C_{H,R}$: Residual hydrogen content.

longitudinal microstructure texture formed in the rolling direction. In this study, Mode II cracks also initiated and propagated along the longitudinal microstructure texture (See Figure 1). Mode I crack growth direction was ± 45° in all tests. This is because Mode I crack growth direction is dependent only on cyclic stress. Mode II crack length was longer under the compression-torsion test than under the pure torsion test. Takahashi and Murakami [8] pointed out that branching from Mode II to Mode I is controlled by local tangential stress ahead of a Mode II crack. Stress amplitude $\sigma_{\theta,a}$ is the same under the pure torsion test (τ_a=900 MPa, σ_m=0 MPa) and the compression-torsion test (τ_a=900 MPa, σ_m=-750 MPa). Mean stress $\sigma_{\theta,m}$ of local tangential stress is zero under the pure torsion test. $\sigma_{\theta,m}$ is compressive under the compression-torsion test. Therefore, $\sigma_{\theta,m}$ delayed the branch from Mode II crack to Mode I crack. As the result, Mode II crack length was longer than under the compression-torsion test, and fatigue life under the compression-torsion test was 2 ~ 10 times longer than that under the pure torsion test.

Two Mode II cracks also coalesced with each other in the hydrogen-pecharged specimen. The critical Mode II crack length was almost the same for the uncharged and the hydrogen-precharged specimens under the compression-torsion test (τ_a=900 MPa, σ_m=-750 MPa).

In the case of the hydrogen-precharged specimen under a pure torsion test, the critical Mode II crack length was very short. This is because the fracture origin was a subsurface inclusion and Mode I crack propagated directly from subsurface inclusion.

Figure 7 shows Mode II cracks taken by the replica method under compression-torsion test (τ_a=900 MPa, σ_m=-750 MPa). The fatigue lives were N_f=1.8×10^5 for the uncharged specimen and N_f=8.8×10^4 for the hydrogen-precharged specimen. Figure 7 (a-1) and Figure 7 (b-1) show replicas just before Mode II crack initiation, Figure 7 (a-2) and Figure 7 (b-2) show replicas just after Mode II crack initiation, Figure 7 (a-4) and Figure 7 (b-4) show replicas at the branch from a Mode II crack to a Mode I crack, and Figure 7 (a-5) and Figure 7 (b-5) show replicas just before failure. Two Mode II cracks also coalesced with each other in the hydrogen-pecharged specimen as shown Figure 7 (b-4). The critical Mode II crack length before branching to Mode I was almost equal: 74 μm for the uncharged specimen and 84 μm for the hydrogen-prechaged specimen. White arrows in Figure 7 (a-5) and Figure 7(b-5) show the branched Mode I crack. The angle of ±70.5 º is calculated by the local maximum nominal stress ($\sigma_{\theta, max}$) criterion [8]. The angle close to ±45 º is the direction perpendicular to the remote maximum principal stress. It is apparent that Mode II crack branches in the direction of ±70.5° and then grew in the direction of ±45°

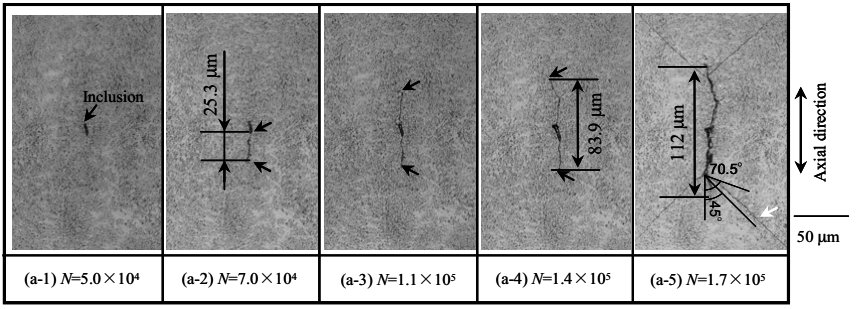

(a) Uncharged, N_f=1.8× 10^5

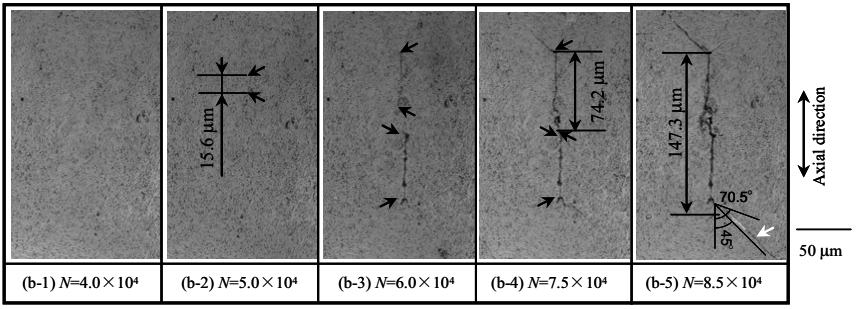

(b) Hydrogen-precharged, N_f=8.8×10^4, $C_{H,R}$=1.52 ppm

FIGURE 7 Fatigue cracks of the uncharged and hydrogen-precharged specimens of the SAE52100 under cyclic torsion with a compressive mean stress (σ_m=-750 MPa, τ_a= 1000 MPa, f=3 Hz). $C_{H,R}$: Residual hydrogen content.

TABLE 2 The number of cycles to failure, N_f, the number of cycles to Mode II crack initiation, $N_{II,i}$, the number of cycles during Mode II, $N_{II,p}$, the number of cycles during Mode I, $N_{I,p}$ for the uncharged and hydrogen-precharged specimens of the SAE52100 (σ_m=-750 MPa, τ_a= 1000 MPa, f=3 Hz).

	N_f	$N_{II,i}$	$N_{II,p}$	$N_{I,p}$
Uncharged	1.8×10^5	7.0×10^4	7.0×10^4	4.0×10^4
Hydrogen-precharged	8.8×10^4	5.0×10^4	2.5×10^4	1.3×10^4

Table 2 shows Mode II crack initiation life, $N_{II,i}$, Mode II crack propagation life, $N_{II,p}$ and Mode I crack propagation life, $N_{I,p}$. $N_{II,i}$ is defined as the number of cycles at Figure 7(a-2) for the uncharged specimen and at Figure 7(b-2) for the hydrogen-precharged specimen. Mode II crack length was not significantly different between the uncharged specimen (25.3 μm) and the hydrogen-precharged specimen (15.6 μm). $N_{II,P}$ is the difference in the number of cycles between Figure 7(a-4) and Figure 7(a-2) for the uncharged specimen, and between Figure 7(b-4) and Figure 7(b-2) for the hydrogen-precharged specimen. $N_{I,P}$ is the difference in the number of cycles between N_f and Figure 7(a-4) for the uncharged specimen, and between N_f and Figure 7(d-4) for the hydrogen-precharged specimen. Table 2 shows that the fatigue crack acceleration due to the hydrogen is 2.8 times for Mode II crack growth and 3.1 times for Mode I crack growth. Therefore, as shown Figure 4(a) and Figure 4(b), the fatigue lives of specimens which fractured from matrix were shorter in the

hydrogen-precharged specimens than in the uncharged specimens under both pure torsion and compression-torsion tests.

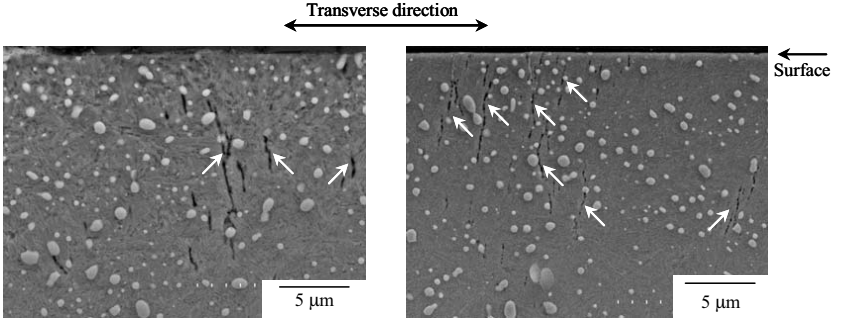

(a) Under cyclic torsion without a compressive mean stress, τ_a= 800 MPa, σ_m=0 MPa, f=3 Hz
N_f=1.7× 10^5, $C_{H,R}$=1.58 ppm

(b) Under cyclic torsion combined with compressive mean stress, τ_a= 900 MPa, σ_m=-750 MPa, f=3 Hz
N_f=3.0× 10^5, $C_{H\cdot R}$=0.79 ppm

FIGURE 8 Microstructural changes at the transverse cross section for the uncharged and hydrogen-precharged SAE52100 under cyclic torsion with and without a compressive mean stress. $C_{H,R}$: Residual hydrogen content.

Figure 8 shows an example of the microstructural changes on the transverse cross section of the hydrogen-precharged specimens in a pure torsion test and a compression-torsion test. Both specimens showed matrix initiation. The transverse cross sections were etched in picral. Fatigue test conditions and lives are included in the figures. Many fibrous microstructural changes were observed at the surface and in the interior near the surface for hydrogen-precharged specimens in both pure torsion and compression-torsion tests. These microstructural changes imply that enhanced slip deformation and localized slip bands due to the hydrogen produce microstructural changes and eventually more mode II fatigue cracks along slip bands in the hydrogen-charged specimens.

Conclusion

To investigate effect of hydrogen on Mode II fatigue behavior of bearing steel (SAE 52100, HV=748) tempered at 438K, fatigue tests were conducted under the cyclic torsion with and without a compressive mean stress. The conclusions can be summarized as follows:

(1) Fracture origin and fracture lives are dependent on the compressive mean stress and hydrogen. Under a pure torsion test, the fracture origin was in the matrix at the surface for the uncharged specimens. The fracture origin was at a subsurface inclusion (Al_2O_3·CaO) for the hydrogen-precharged specimens. It is presumed that hydrogen enhanced concentration of plastic deformation at subsurface inclusion and crack initiation followed by Mode I fracture. Fatigue lives N_f in the hydrogen-precharged specimens were shorter by a factor of more than 1/10 compared to those in the uncharged specimens.

(2) Under a compression-torsion test, the fracture origin was at a surface inclusion (TiN) for the uncharged specimens. This is because interface between an inclusion and a matrix is debonded due to the coupled effect of the compressive mean stress and cyclic stress, and then Mode II crack initiated from debonded interface. The fracture origin was in the matrix for the hydrogen-precharged specimens. This is because the hydrogen enhanced localized slip deformation.

(3) Mode II fatigue crack growth rate and Mode I fatigue crack growth rate in the hydrogen-precharged specimen were higher than those of uncharged specimen under the

compression-torsion test. As a result, the fatigue lives were shorter by a factor of more than 1/2 in the hydrogen-precharged specimens than in the uncharged specimens.

(4) More mode II fatigue cracks and microstructural changes were observed in the hydrogen-precharged specimens than in the uncharged specimens. This is due to the hydrogen enhanced slip localization on the specimen surface.

(5) Mode II crack length and fatigue lives in the uncharged and the hydrogen-precharged specimens were longer under the compression-torsion test than under the pure torsion test. That the compressive mean stress acts on Mode I crack face under the compression-torsion test and delays the branching from Mode II to Mode I.

(6) Mode II fatigue cracks in the uncharged and hydrogen-precharged specimens initiated and propagated along the axial direction due to the longitudinal microstructure texture formed in the rolling direction. Finally, Mode II cracks branched into two Mode I cracks.

Acknowledgment

This research has been supported by the NEDO Fundamental Research Project on Advanced Hydrogen Science (2006 to 2012)

References

[1] Murakami, Ya., Naka, M. and Iwamoto, A., *SAE Technical Paper*, 950944, (1995), pp.1-14.

[2] Becker, P. C., Metals Technology, Vol.8, No.6 (1981), pp. 234-243.

[3] Harris, T., A. and Kotzalas, M., N., Rolling Bearing Analysis, *CRC Press*, Fifth Edition, (2007), pp.295-299.

[4] Iso, K., Yokouchi, A. and Takemura, H., *SAE Technical Paper*, 2005-01-1868.

[5] Murakami, Y. and Nagata, J., *Journal of the Society of Materials Science, Japan* Vol.54, No.4 (2005) pp. 420-427.

[6] Uyama, H., Mine, Y., Murakami, Y., Nakashima, M. and Morishige, K., *Fatigue & Fracture of Engineering Materials and Structures*, Vol.29 (2006), pp.10616-1074.

[7] Zhang, A. and Akid, R., *Fatigue & Fracture of Engineering Materials and Structures,* Vol.20, No.4 (1997), pp.547-557.

[8] Takahashi, K. and Murakami, Y., *Transactions of the Japan Society of Mechanical Engineers. A*, Vol.68, No.668 (2002) pp. 645-652.